Techniques in Coloproctology (2019) 23:53–63
https://doi.org/10.1007/s10151-018-1914-y

MULTIMEDIA ARTICLE

Robotic-assisted stereotactic real-time navigation: initial clinical experience and feasibility for rectal cancer surgery

S. Atallah[1] · E. Parra-Davila[2] · A. G. F. Melani[3] · L. G. Romagnolo[4] · S. W. Larach[1] · J. Marescaux[5]

Received: 5 December 2018 / Accepted: 15 December 2018 / Published online: 17 January 2019

Abstract

Background Real-time stereotactic navigation for transanal total mesorectal excision has been demonstrated to be feasible in small pilot series using laparoscopic techniques. The possibility of real-time stereotactic navigation coupled with robotics has not been previously explored in a clinical setting.

Methods After pre-clinical assessment, and configuration of a robotic-assisted navigational system, two patients with locally advanced rectal cancer were selected for enrollment into a pilot study designed to assess the feasibility of navigation coupled with the robotic da Vinci Xi platform via TilePro interface. In one case, fluorescence-guided surgery was also used as an adjunct for structure localization, with local administration of indocyanine green into the ureters and at the tumor site.

Results Each operation was successfully completed with a robotic-assisted approach; image-guided navigation provided computed accuracy of ±4.5 to 4.6 mm. The principle limitation encountered was navigation signal dropout due to temporary loss of direct line-of-sight with the navigational system's infrared camera. Subjectively, the aid of navigation assisted the operating surgeon in identifying critical anatomical planes. The combination of fluorescence with image-guided surgery further augmented the surgeon's perception of the operative field.

Conclusions The combination of stereotactic navigation and robotic surgery is feasible, although some limitations and technical challenges were observed. For complex surgery, the addition of navigation to robotics can improve surgical precision. This will likely represent the next step in the evolution of robotics and in the development of digital surgery.

Keywords Digital surgery · TaTME · Rectal cancer · Robotic colorectal · Augmented reality · Da Vinci navigation · Stereotactic navigation · Image-guided surgery · Fluorescence-guided surgery

Introduction

Although utilized principally in the fields of neurological surgery, otolaryngology, and orthopedic surgery, frameless stereotactic navigation has been successfully applied

Electronic supplementary material The online version of this article (https://doi.org/10.1007/s10151-018-1914-y) contains supplementary material, which is available to authorized users.

✉ S. Atallah
atallah@post.harvard.edu

E. Parra-Davila
eparradavila@gmail.com

A. G. F. Melani
armandomelani@icloud.com

L. G. Romagnolo
drluisromagnolo@gmail.com

S. W. Larach
swlarach@aol.com

J. Marescaux
Jacques.marescaux@ircad.fr

1 Department of Colorectal Surgery, EndoSurgical Center of Florida, Florida Hospital, 100 N. Dean Road, Orlando, FL 32825, USA

2 Department of Surgery, Good Samaritan Hospital, West Palm Beach, FL 33401, USA

3 Department of Surgery, IRCAD, Latin America, Rio de Jeneiro, Brazil

4 Department of Surgery, IRCAD, Latin America, Barretos, Brazil

5 Department of Surgery, IRCAD, France, Strasbourg, France

clinically for more than a quarter century [1–3]. The feasibility of navigation for soft tissue anatomic targets such as the rectum has previously been described for transanal total mesorectal excision (taTME), whereby frameless stereotactic navigation was utilized to provide real-time position assessment during the transanal portion of the operation with considerable accuracy [4–8]. Such image-guided surgery has also been employed to assist in the en bloc resection of pelvic neoplasia [9, 10]. In small studies, these novel approaches have been demonstrated to be both feasible and accurate, providing navigational accuracy of approximately ± 4 mm.

Over the past two decades, robotic soft tissue surgery including colorectal resection has been developed, refined, and even redefined [11, 12]. New applications have included robotic taTME [13–16]. The impetus for this has been to optimize the quality of surgery through improved access and precision [17, 18]. While a variety of innovative robotic platforms lurk along the near horizon [19], the vast majority of robotic surgery experience has been gained using a single system – the da Vinci surgical system (Intuitive Surgical, Sunnyvale, CA, USA). A variety of ingenuous and quite innovative models using TilePro [20] have been developed, primarily in a pre-clinical setting, aimed at integrating augmented reality and image-guidance for non-colorectal applications [21–27]. Stereotactic navigation coupled with robotic surgery is a new concept, and we have recently described a protocol which could be feasible, although technically challenging [28]. Until now, an interface between real-time stereotactic navigation and da Vinci robotics has not been established due to a variety of technical factors and challenges. Here, the first human cases of robotic navigation are reported as applied to radical rectal cancer resection via both the abdominal and transanal approaches. The manuscript is supplemented with multimedia video content available online.

A construct for navigation in robotic surgery

A detailed approach to navigation for rectal cancer surgery has been described previously [4, 5, 7, 8], including pre-clinical experimentation with the robotic platform [28]. This is only briefly reviewed here. Compulsory elements for live, real-time navigation include (a) an instrument tracker, (b) a fixed-point patient tracker, (c) body imaging performed with radio-opaque markers (fiducials), and (d) an infrared camera (which must maintain direct line-of-sight with both the patient and instrument trackers), and (e) specialized navigational software. When properly configured, a digital coordinate system representing digital space DS, (X_{DS}, Y_{DS}, Z_{DS}) corresponds to a coordinate system in real space RS, (X_{RS}, Y_{RS}, X_{RS}) with millimetric accuracy.

To perform navigation with the da Vinci *Xi* surgical system, an instrument tracker (which can be sterilized, and which is configured with a reference array) is secured firmly with a screw and bracket to the robotic instrument shaft at its proximal end, near the instrument housing. The tracker includes the option of either three or four tracker spheres (i.e. reference array) that correlate RS with DS. The reference array must be able to rotate freely along the axis of the robotic instrument's 8 mm shaft since the shaft rotates with wrist movements during master–slave operation, and during the initial instrument registration process upon inserting the instrument. The instrument tracker's reference array must also maintain direct line-of-sight with a mounted infrared antenna for real-time tracking (Fig. 1). After a calibration process, the robotic instrument's scissor tip relative to the tracker spheres is determined and thus the dissecting instrument's DS position is constantly known during operation.

Typically, the navigational map is either a digital computed tomogram or data obtained from magnetic resonance imaging. Both formats can be used to construct a three-dimensional (3D) rendering of the anatomy to be navigated, which can be manipulated in space, or using multi-planar rendering. For improved accuracy, it is recommended that body imaging is obtained immediately before surgery or, when possible, intraoperatively [4]. The imaging for navigation is obtained with skin-fixed fiducials (objects placed in the field of view of an imaging system which appears in the image produced, for use as a point of reference or a measure). By determining the exact fiducial positions overlying the area to be navigated, the actual patient's position in RS is known relative to DS, allowing for navigation to take place. This also requires a patient tracker, which, in this case, is bedrail mounted and which cannot move relative to the patient without disrupting the accuracy of the navigational data.

Preparation and pre-clinical experimentation

Consecutive dry laboratory sessions were conducted utilizing the da Vinci Robotic surgical system coupled with a commercially available navigational system (StealthStation S8 surgical navigation system, Medtronic, Inc., Minneapolis, MN, USA). While the StealthStation S8 is designed primarily for neurological and spine surgery, the software can be configured to navigate alternate targets, including soft tissue organs (such as the rectum and mesorectum) and other fixed pelvic anatomy. However, for the purpose of system testing, a model of a human face was used. In this dry lab construct, a plastic model of a human head, which correlated to a 3D reconstructed magnetic resonance imaging (MRI). The aim of this pre-clinical

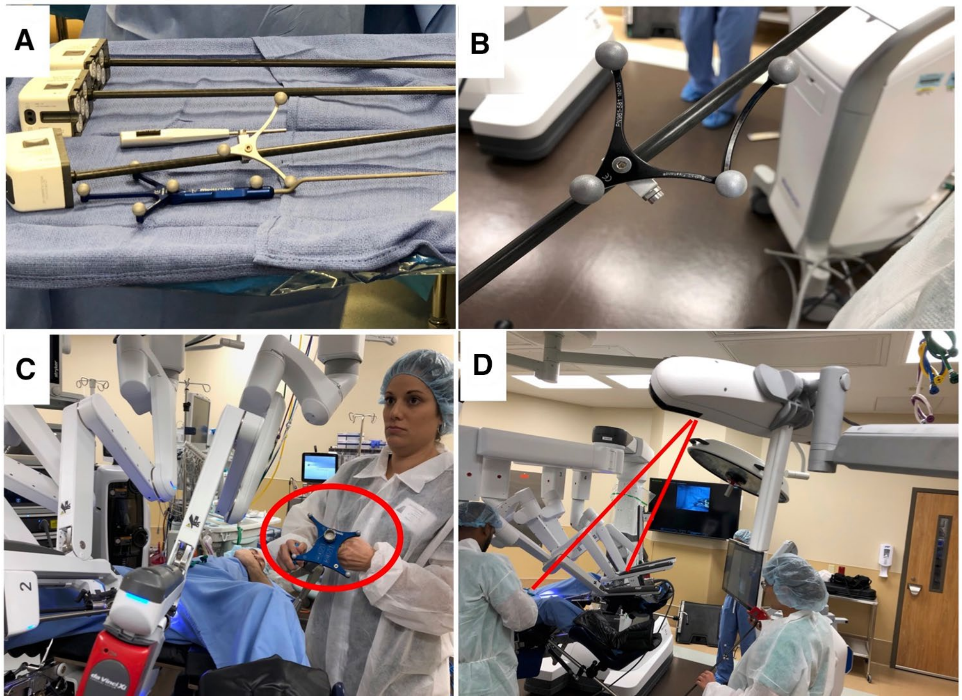

Fig. 1 Navigation in surgery requires specialized software, and specific hardware that must be properly configured prior to surgery. **a** A three-sphere reference array, or instrument tracker, has been secured to the shaft of an 8 mm *Xi* robotic scissor tip near to the housing. A special ‘pointer’ (blue with silver spheres) is used to calibrate the device and to ‘teach’ the system where the actual anatomy lies in three-dimensional space, which also requires the scan to be completed with skin-fixed fiducials. **b** An optional four-sphere reference array is secured to the robotic instrument shaft. **c** The bedrail mounted, adjustable four-sphere patient tracker provides a frame of reference for the patient’s position in space. After calibration, movement of the patient is not possible without loss of navigational precision. **d** A specialized infrared camera must maintain direct line-of-sight with the instrument being tracked (instrument tracker) and the patient tracker to maintain real-time navigation during robotic surgery

experiment was to test the feasibility of robotic surgery coupled with navigation. The navigational system and the robotic platform were interfaced via a digital HDMI connection and the TilePro feature allows viewing of navigational real-time data on the surgeon’s console, which could be interpreted together with the optical (stereoscopic) video. In this manner, a surgeon is able to interpret anatomy by video from a single vantage point simultaneously with a 3D reconstructed map viewable from any vantage point (Fig. 2). The computed accuracy achieved in pre-clinical testing was ± 3.4 mm. The digital interface between the robotic console allowed for a clear representation of the navigational map, with an uninterrupted ability to assess scissor tip position. Accuracy was maximized when the scissor tip wrist was ‘straight’ reflecting its natural position.

Institutional review board approval was then obtained for a pilot study designed to assess the feasibility of robotic navigation for rectal cancer surgery in a clinical setting. Specifically, robotic-assisted navigation for taTME and anterior resection were conducted.

Clinical case 1: Robotic taTME with navigation for rectal cancer

The patient was a 68-year-old female, body mass index (BMI) 19.2 kg/m^2, who had presented with large bowel obstruction secondary to locally advanced, biopsy-proven adenocarcinoma of the distal one-third of the rectum. The patient had proximal diversion of the fecal stream with a transverse loop colostomy and appropriate staging, which revealed no evidence of metastatic disease. MRI showed a mid-rectal tumour, 4.9 cm in craniocaudal diameter, cT3N1, 4.5 cm from the anal verge. The patient reveived long-course neoadjuvant treatment. The protocol consisted of 5-fluoropyrimidine based chemotherapy (oral Capecitabine) with concurrent external beam radiotherapy to 50.4 Gy, administered in 28 fractions. After a 10-week resting period, robotic taTME was performed with real-time stereotactic navigation (Fig. 3).

Immediately prior to surgery, 20 skin-fixed fiducials were placed over the lower pelvis in a curve-linear fashion from the anterior superior iliac spine bilaterally, overlying

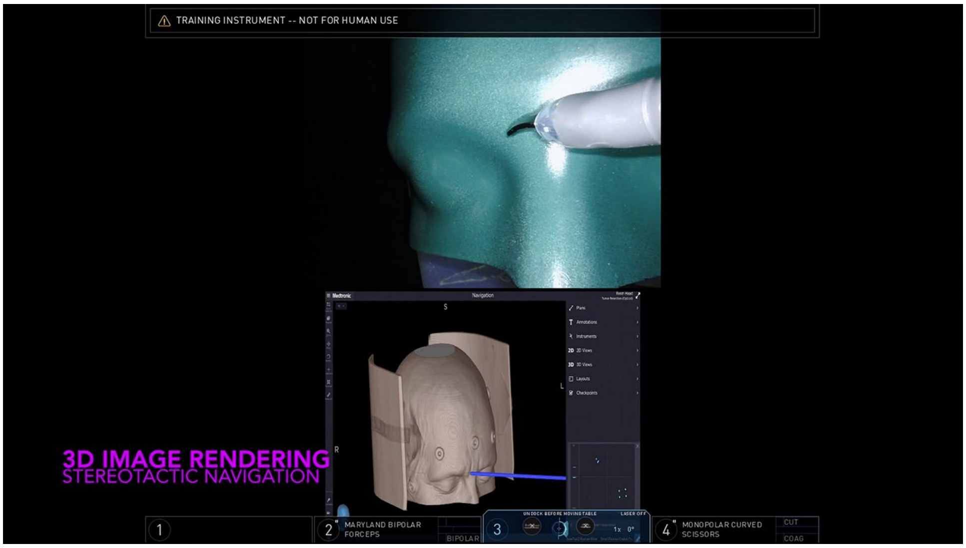

Fig. 2 Shown is the surgeon's console view from the da Vinci *Xi* terminal. A plastic model of a human face (green) was used in this pre-clinical model for the purpose of assessing the feasibility and connectivity of navigation with robotics. Utilizing the TilePro feature, a second image is projected onto the console, which has been configured to be viewed beneath the optical video feed. The 3D rendition of the actual plastic model is illustrated, and this can be manipulated to view any vantage point in digital space. The da Vinci scissor tip is the instrument being tracked and its trajectory and tip position is tracked in real-time (blue wand) during the process of navigation. Computed accuracy measured ± 3.4 mm during pre-clinical testing

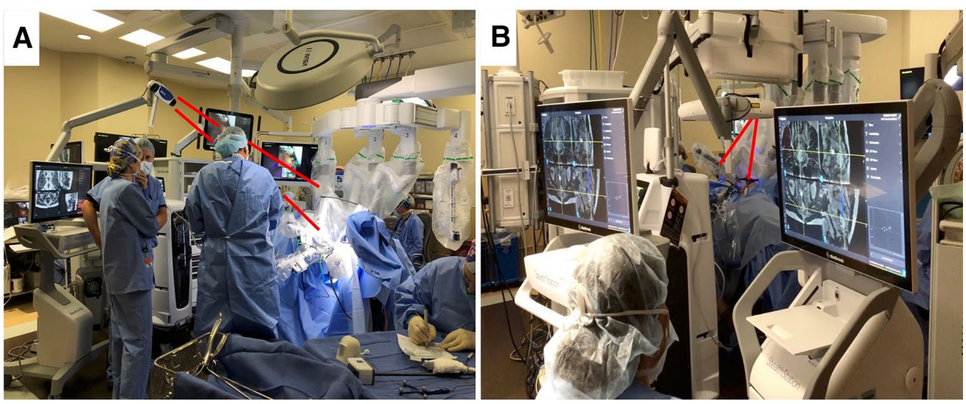

Fig. 3 The general configuration is shown for two clinical cases completed with robotic-assisted surgery coupled with stereotactic navigation. **a** Robotic taTME with the used of 3 robotic instruments. An overhead infrared (IR) camera constantly determines the position of the instrument being tracked (robotic scissor tip) and where the data is displayed on LCD monitors and at the surgeon console. Direct line-of-sight between patient tracker and IR camera, as well as the instrument tracker and IR camera (red lines) are required. **b** The IR camera tracks the position of the patient and instrument tracker during robotic-assisted TME (red lines denote line-of-sight)

the pubic symphysis, in a 'bikini-like' pattern (Fig. 4). Next, the patient underwent a rectal protocol MRI, and this scan was imputed into the StealthStation so as to construct a navigational map. The patient tracker was secured to the bedrail and a four-sphere instrument tracker was attached to the proximal end of the scissor tip. The instrument tracker was then calibrated, and a pointer was used to register each of the skin fiducials (a process termed patient-to-image registration), allowing the patient's position in *RS* to correlate with the navigational map, *DS* (Fig. 5). The software minimum acceptable accuracy tolerance was set to ± 5 mm, and the actually computed navigational accuracy was computed to measure ± 4.5 mm. The sequence of surgery for this case was as follows: (a) diagnostic laparoscopy was first performed to exclude distant metastatic disease, (b) robotic taTME with stereotactic navigation was next performed to the level of the peritoneal reflection (Fig. 6a, b), then, working with only a single team, (c) the left colon and splenic flexure was mobilized laparoscopically using the medial-to-lateral technique, including

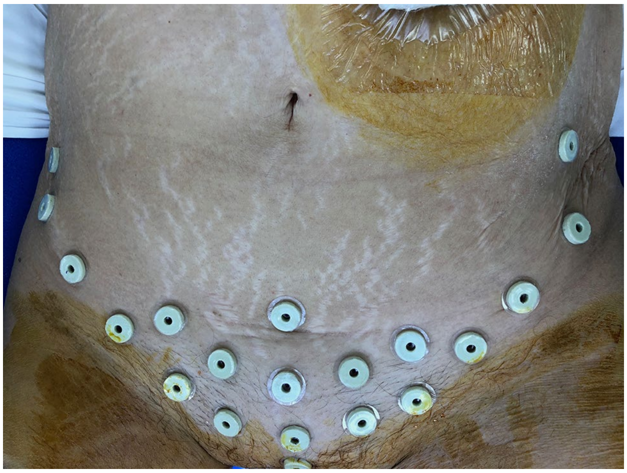

Fig. 4 Twenty skin-fixed fiducials were placed in a 'bikini-like' pattern overlying the low pelvis. Body imaging used for navigation is performed with these radio-opaque markers which is important for the registration process that will correlate digital space (DS) with real space (RS). It is important that fiducials are placed near the target to be navigated and that they remain in the same fixed position as when the imaging was obtained

division of the inferior mesenteric vein and artery. Finally, (d) the mobilized specimen was extracted via a small pfannensteil incision, resected extra-corporeally, and delivered back into the abdominopelvic cavity where a hand-sewn coloanal anastomosis was performed. Note that navigation was only utilized during portions of (b), during the critical points of the robotic taTME dissection.

During navigation, correlation between the visualized anatomy, RS, and the navigation map, DS, was observed allowing the operating surgeon to perform the resection under stereotactic guidance. The principle limitation for achieving navigation for robotic taTME was the loss of signal from the instrument tracker, as the tracker spheres, affixed to the spinning robotic instrument shaft, would rotate away from the infrared (IR) camera. To regain the signal, the surgeon would need to rotate the scissor tip until the signal was re-established and line-of-sight was thus restored. Factors increasing hindrance of line-of-sight also included the patient's own anatomy, the bedside assistant, and the robotic drapes. The latter had to be specifically managed and tightened along the robotic arm of the instrument being navigated to avoid encroachment, so that the tracker was able to rotate along the long axis unencumbered.

The resected specimen revealed an intact mesorectal envelope (TME complete), with negative distal and circumferential margins; the tumor was consistent with a mucinous adenocarcinoma measuring 5.0 cm in diameter, with final stage ypT3N2b. There was no intraoperative or postoperative morbidity and the patient's postoperative course was unremarkable.

Clinical case 2: Robotic anterior resection with navigation and organic dye target localization for rectal cancer

The patient was a 36-year-old male, BMI 25.1 kg/m^2, who was diagnosed with a locally advanced, biopsy-proven

Fig. 5 Shown is a multi-planar (axial, coronal, and sagittal) images simultaneously depicting the tracked instrument's tip in real-time during rectal cancer surgery. The instrument is represented by a blue wand, and the cross-hair point represents the tip's actual position as dissection, in this example, proceeds in vivo along the mesorectal envelope. This information can then be translated to the surgeon's console via TilePro for real-time robotic navigation

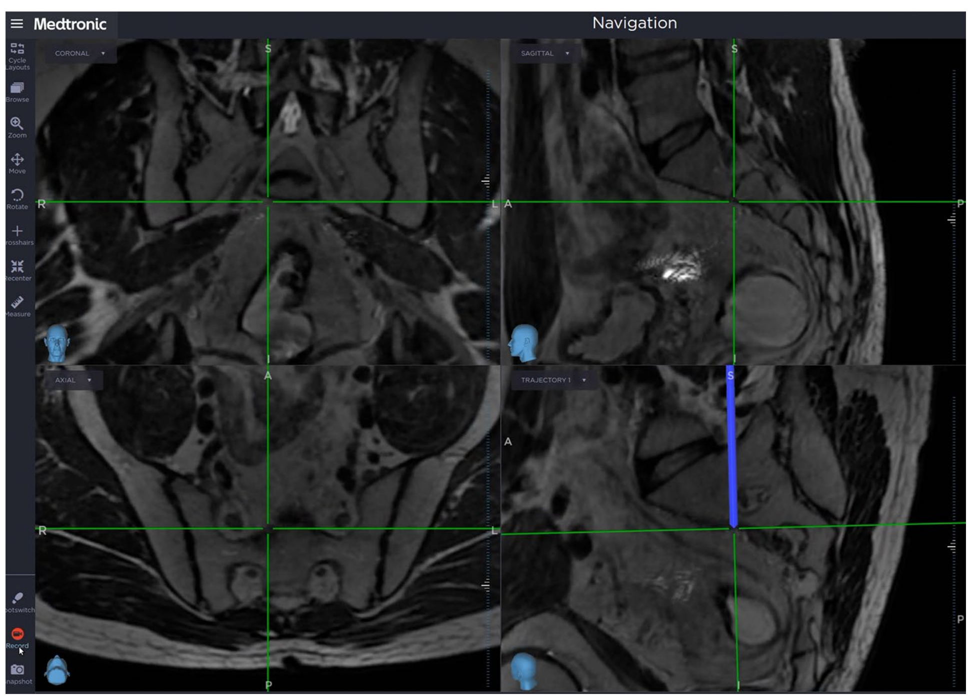

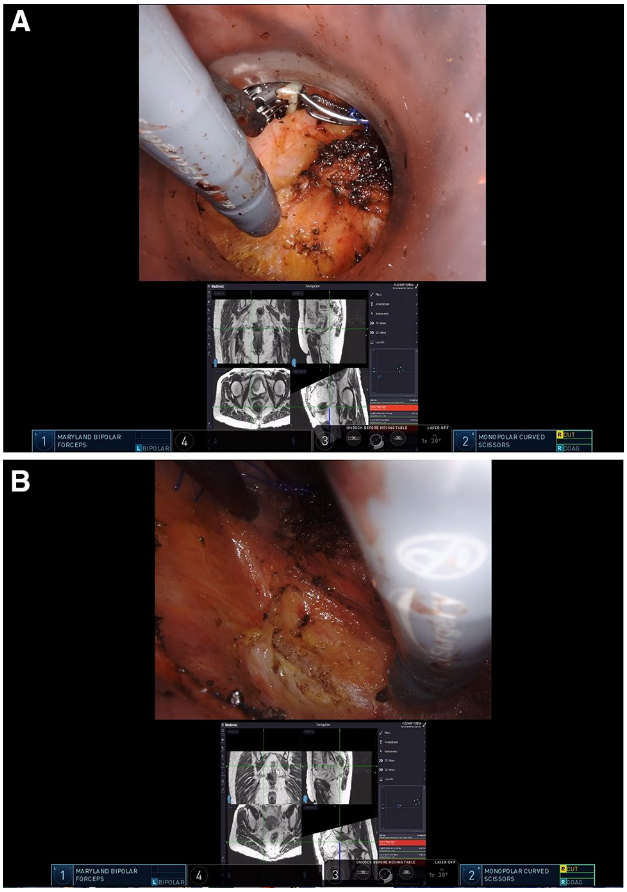

Fig. 6 **a, b** Robotic taTME with real-time stereotactic navigation is shown using the *Xi* robotic platform and TilePro, 3D video with correlating navigational MRI map are displayed. **a** Right lateral dissection (mid-rectum) **b** surgeon's view at the console during posterior dissection; cross-hairs reflect robotic scissor tip position

moderately differentiated rectal adenocarcinoma. The lesion was positioned anteriorly near the peritoneal reflection. The patient received neoadjuvant treatment with oral capecitabine and concurrent external beam radiotherapy to 50.4 Gy administered in 26-fractions. After an 11-week resting period, robotic-assisted, site-specific TME was performed using the da Vinci *Xi* robotic system in combination with stereotactic navigation. On post-treatment MRI, the distal extent of the tumor was 10.5 cm from the anal verge and 7.3 cm from the anorectal ring, straddling the peritoneal reflection. The tumor measured 2.2 cm craniocaudally, staged as cT3N0.

Immediately before surgical resection, the patient had a navigation-protocoled MRI. As in the clinical case above, skin-fixed fiducials were placed over the lower pelvis in a bikini pattern. The advantage of placement of fiducials in this position are twofold. First, the fiducials directly overly the area to be navigated. Next, they are placed in a region that has little movement with either ventilation or abdominal cavity insufflation.

Data from the completed MRI scan was then uploaded into the navigational system, where software was used to render a 3D and multi-planar map of the area to be navigated. The patient tracker was secured, and the instrument tracker was mounted to the robotic instrument and calibrated. Prior to dissection, bilateral ureteral of indocyanine green (ICG) (total of 2.5 ml per ureter) was injected retrogradely via cystoscopy. A colonoscope was also used to inject ICG into the submucosal plane at the distal aspect of the lesion. In this manner, both ureters and the tumor could be localized during robotic stereotactic TME utilizing biofluorescence and an infrared camera (FireFly™ Imaging for da Vinci, or the Stryker AIM 1588 Platform for fluorescence imaging) (Fig. 7). The navigational system was then tested with computed accuracy of ±4.6 mm.

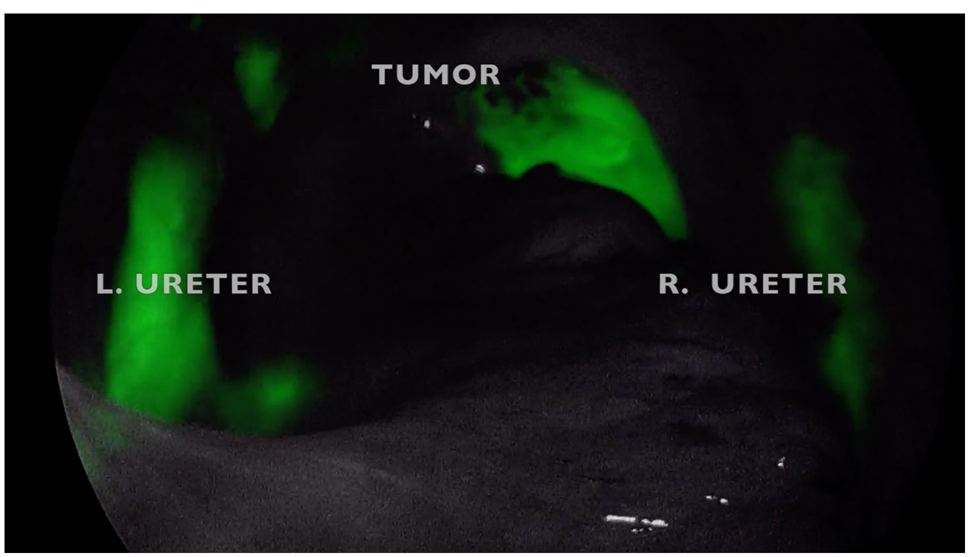

Fig. 7 A view of the pelvis prior to dissection and subsequent to application of ICG for ureteral and tumor localization. Immediately prior to surgery, ICG is infiltrated into the bilateral ureters retrograde, while the tumor is injected in the submucosal plane via flexible endoscopy. Organic dyes can be used to localize structures of interest, providing the surgeon with an augmented understanding of key anatomic structures

In this case, the splenic flexure was mobilized laparoscopically (by surgeon preference). The left ureter was identified by fluorescence imaging. Once the flexure was released, the da Vinci *Xi* robotic cart was position for the anterior dissection. The dissection proceeded with the surgeon able to utilize stereotaxy, optical 3D video, infrared fluorescence for structure localization, either simultaneously or interchangeably. The TilePro feature allows for a size-customizable second viewing window which allowed the surgeon to optimize the console configuration to personal preference. As with robotic taTME with navigation, stereotaxy was used during the most critical portions of the operation, most notably, along the anterior dissection of the tumor which straddled the peritoneal reflection (Fig. 8). By utilizing navigation in combination with ICG for structure localization, the surgeon's perception of the dissection plane was augmented (Fig. 9).

The resected specimen revealed a completely intact mesorectal envelope negative distal and circumferential margins; the tumor was consistent with a mucinous adenocarcinoma measuring 1.5 cm in diameter, with final stage ypT1N0. There was no intraoperative or postoperative morbidity and the patient's postoperative course was uneventful. Both cases 1 and 2 are detailed in the supplemental multimedia content available online.

Discussion

Frame-based navigation in surgery was introduced by Spiegel et al. in 1947 [29], and subsequently, in 1986, Roberts et al. introduced frameless navigation [2], which remains the foundation of modern surgical navigation today. According to Willems et al. [30], navigation is essentially a 3D digitizer which correlates measurements to a reference data set, and whose objective is threefold: (a) to define a coordinate space for the imaging map, and also one for the surgical field, (b) to determine the special relationship between these coordinate spaces, and (c) present the surgeon with usable information determined from an understanding of this spatial relationship.

Although randomized controlled trials which examine outcomes with and without navigation during surgery are sparse [31], there is encouraging data to suggest its benefit. For example, in a study by Wirtz et al., 52 patients having radical resection of intracranial glioma with navigation was compared against matched historical controls performed without navigation [32]. The analysis revealed that the radiologic radicality (based on postoperative MRI) was more likely to be achieved with navigation than without (31% vs. 19%) and a trend towards prolonged survival with navigation was observed (13.4 vs. 11.1 months). Corroborating these findings, Kurimoto et al. examined more than a decade of surgical outcomes for adult patients with supratentorial

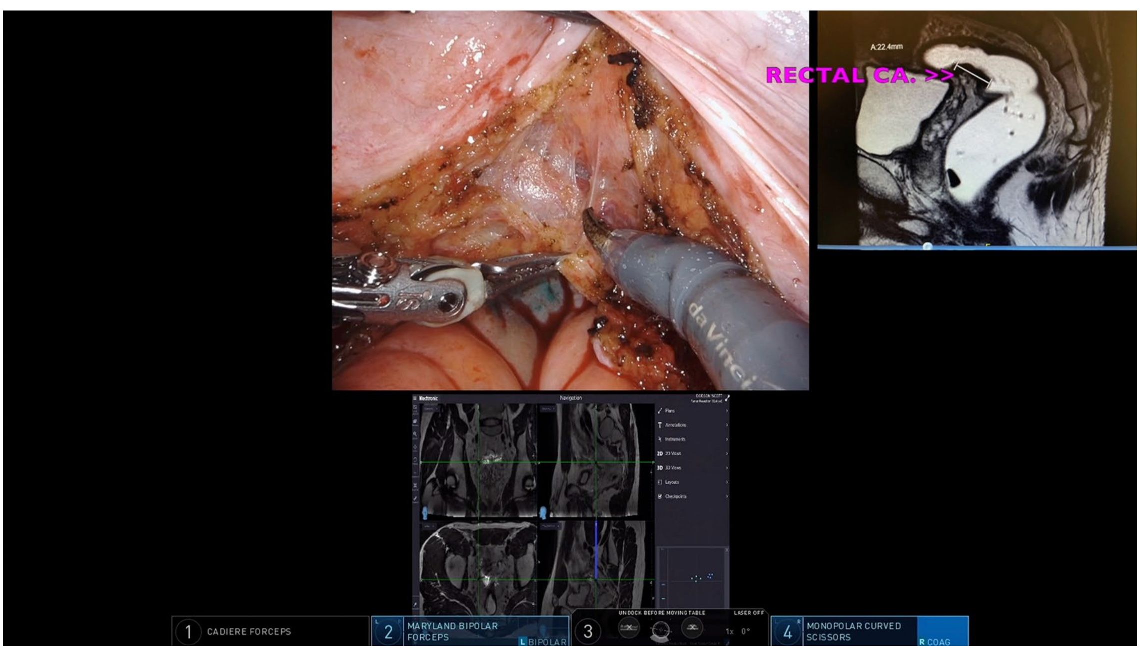

Fig. 8 Console view of robotic-assisted, site-specific TME being performed with real-time stereotactic guidance. The tattooed anterior rectal tumor straddles the reflection and is here being dissected free of the seminal vesicles and vas deferens along the proximal extent of Denonvilliers' (retroprostatic) fascia

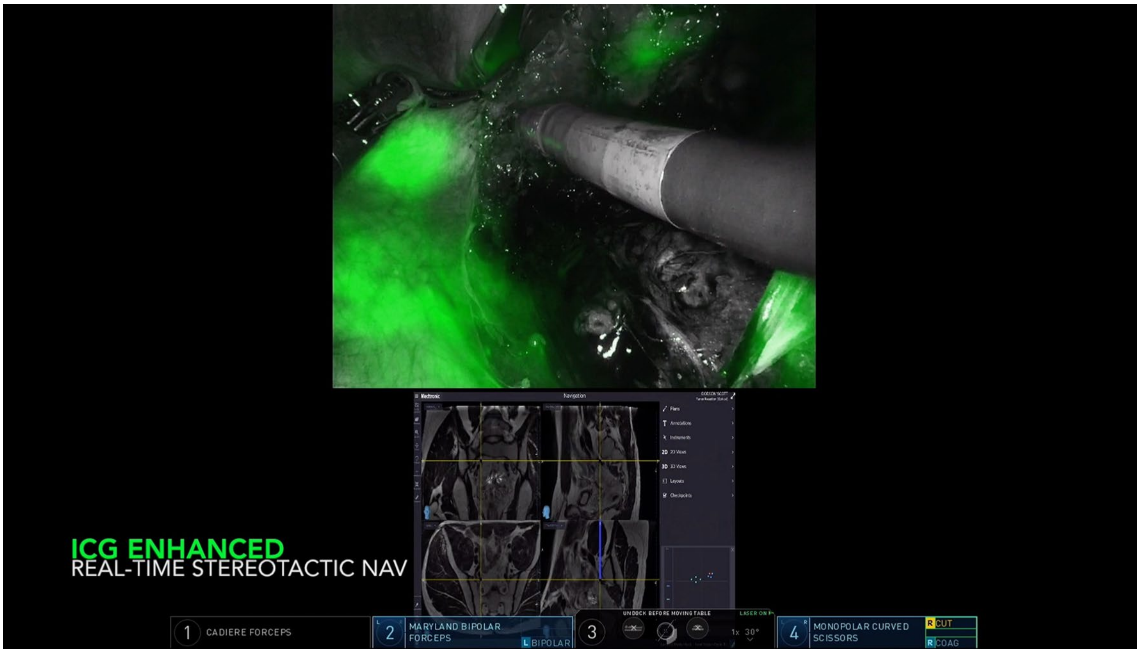

Fig. 9 Using the da Vinci FireFly™ mode, the left ureter and tumor are localized, thereby delineating their relative position during surgery. Simultaneously, real-time stereotactic navigation is used to create an augmented operating environment. Here, the left lateral dissection, in close proximity to the tumor, is being performed

malignant astrocytomas, with 42 of the 76 resections performed with navigation [33]. The results demonstrated that the lesions were more likely to be completely removed with the aid of navigation (64.3% vs. 38.2%, $p < 0.05$), and that this translated in to a near doubling of median survival (16 vs. 9 months).

While there are inherent limitations of transposition, these data suggest that a more precise and complete oncologic resection can be achieved with navigation, and that oncological completeness may, in turn, translate into improved clinical outcomes. In our quest for precision in rectal cancer surgery [34, 35], and as robotics in surgery becomes increasingly digitized, the next step in the evolution of robotics will likely encompass image-guided modules which will augment the surgeon's understanding of complex anatomic structures [36]. This first-in-human pilot study is demonstrative of the potential for science to meld the mechanical-based advancements in surgical instrumentation with computer-based advancements in imaging and navigation, thereby rendering an enhanced operative environment.

In this pilot study, determining feasibility of navigation for rectal cancer surgery was the primary objective. Observed navigation accuracy measured < 5 mm and was calculated to be ± 4.5 mm to 4.6 mm during the periods in which navigation was utilized during the critical portions of surgery (i.e., dissection near the tumor). While both patients had adequate oncologic clearance of disease, no conclusion about the benefit or potential clinical value of navigation in robotics for rectal cancer surgery can be determined based on this feasibility study. In addition, although navigation coupled with robotics was here demonstrated to be possible, there were important limitations (Table 1). First, a technical limitation was encountered due to loss of sight between the instrument tracker and the infrared camera. This occurred

Table 1 Important limitations and challenges for robotic stereotactic navigation

1. Loss of line-of-sight with IR camera
Drapes obscure line-of-sight
Wrist movement of robotic scissor tip causes rotation of instrument tracker's reference array away from the camera
2. Instrument's natural tip motion away from the neutral position relative to the long axis results in inaccuracies in navigation
3. Patient tracker movement, or patient movement due to diaphragmatic excursion, insufflation, or sacral movement after calibration
4. Fiducial and patient tracker placement, if not overlying the area to be navigated, can result in diminished navigation accuracy
5. Mobilized structures are no longer reflected by the navigational map created prior to surgical dissection

secondary to the rotation of the instrument shaft along the long axis which lead to loss of signal and a 'drop out' of real-time navigation. Additionally, direct line-of-sight was lost when the robotic disposable drape obscured one or more of the reference array's tracker spheres from view of the infrared camera. Second, the robotic scissor tip was calibrated with the wrist in the neutral position. Thus, any degree of scissor tip motion away from 0° would result in an inherent loss in navigation accuracy. Third, any movement of the patient anatomy in the region being navigated relative to the patient tracker would render the navigational map less precise, whereby DS ≠ RS. Importantly, the area to be navigated should remain in the same position during the registration process as when the preoperative imaging was obtained. Movement of the patient secondary to diaphragmatic excursion, hip flexion, and pneumatic insufflation all define real challenges for preserving the precision in navigational accuracy for minimally invasive rectal cancer surgery [7]. The final limitation of navigation is that once the anatomic target has been mobilized, it is no longer represented by the anatomical (digitized) map used for navigation. While real-time ultrasound based navigation and electromagnetic organ tracking may provide a solution [37–39], their utility remains to be explored.

This research also examined the value of biofluorescence for structure localization, where anatomic targets (namely the primary tumor and the bilateral ureters) were identified. This represents a step toward the development of comprehensive and integrated surgical system which will include source data from a variety of inputs, thereby enhancing the surgeon's perception of the surgical field during complex operations. Currently in the field of colorectal surgery, most clinical experience is with a single organic dye (namely, ICG) and the majority of experience stems from perfusion assessment of the conduit (especially with left-sided resections, including taTME) upon systemic delivery of the dye and subsequent infrared camera detection [40–43]. However, this and alternate organic dyes can be injected locally to delineate specific anatomic targets of interest [44–46]. Due to their unique translucency properties, biofluorescent dyes allow a surgeon to visualize deep structures and to see beyond white light, and thus beyond the surface of a surgical plane [47].

Fluorescence-guided surgery remains an area of ongoing research, with very encouraging results for tumors that exhibit affinity for organic dyes [48]. Perhaps the best example of this is 5-aminolevulinic acid (5-ALA), which when administered orally leads to intracellular accumulation of fluorescent porphyrins in malignant glioma cells. In a randomized controlled multicenter phase III trial, fluorescence-guided surgery with 5-ALA led to increased rates of tumor resection (65% vs. 36%), and a significantly higher progression free survival than tumors operated without fluorescent navigation (41% vs 21.1%) [49], with findings recently corroborated by a 7-year study [50]. While an organic dyes specific to colon and rectal neoplasms has yet to be applied clinically, several investigators have begun to elucidate fluorescent markers which could someday provide clinical application similar to that observed with 5-ALA for glioma resection [51, 52], providing a gateway for tumor localization of adenocarcinoma during colorectal surgery.

The advancements described herein, and developments described by others, are harbingers of a new era in surgery, where computer-assisted systems (including navigation) will be fused with minimally invasive and robotic instrumentation [19, 27, 36, 53–57]. Many refer to this as the digitization of surgery, or more simply digital surgery. Globally, this is a small step toward future development of comprehensive and integrated surgical systems which will include usable source data from a variety of inputs.

Acknowledgements The authors wish to thank Laura Galorneau, Zack Demetriou, Meraj Baig, Tina Langaee, Meghann Vizintos, Janelle Abravaya, Brian Solomon, and Lauren Skesavage for there assistance with this research.

Funding No funding was received for this study.

Compliance with ethical standards

Conflict of interest Dr. S. Atallah reports consultancy (such as consulting fees, honoraria) from Medtronic, Applied Medical, ConMed, Inc, and Medrobotics. Dr. S. Larach holds stock options with Applied Medical. Dr. J. Marescaux is president of both IRCAD and IHU Strasbourg, which are partly funded by Karl Storz, Medtronic, and Siemens Healthcare though he has no direct conflict of interest with content discussed in this manuscript. Dr. A.G.F. Melani receives remuneration (payment for services not otherwise identified as salary such as consulting fees, honoraria) from Medtronic, Ethicon, Intuitive Surgical, and Verb Surgical though he has no direct conflicts of interest with content discussed in this manuscript. Dr. E. Parra-Davila receives remuneration (payment for services not otherwise identified as salary such as consulting fees, honoraria) from Medtronic, Ethicon, Intuitive Surgical, and Verb Surgical though he has no direct conflicts of interest with content discussed in this manuscript. Dr. L. Romagnolo has received remuneration (honoraria) from Medtronic, Inc. and Johnson & Johnson.

Ethical approval This research was performed in accordance with the ethical standards of the institutional and/or national research committee and with the 1964 Helsinki declaration and its later amendments or comparable ethical standards.

Informed consent Informed consent was obtained in accordance with the standards set forth by hospital regulations.

References

1. Mezger U, Jendrewski C, Bartels M (2013) Navigation in surgery. Langenbecks Arch Surg 398:501–514

2. Roberts DW, Strohbehn JW, Hatch JF, Murray W, Kettenberger H (1986) A frameless stereotaxic integration of computerized tomographic imaging and the operating microscope. J Neurosurg 65(4):545–549
3. Barnett GH, Kormos DW, Steiner CP, Weisenberger J (1993) Intraoperative localization using an armless, frameless stereotactic wand. J Neurosurg 78(3):510–514
4. Atallah S, Nassif G, Larach S (2015) Stereotactic navigation for TAMIS-TME: opening the gateway to frameless, image-guided abdominal and pelvic surgery. Surg Endosc 29(1):207–211
5. Atallah S, Martin-Perez B, Larach S (2015) Image-guided real-time navigation for transanal total mesorectal excision: a pilot study. Tech Coloproctol 19(11):679–684. https://doi.org/10.1007/s10151-015-1329-y
6. Atallah S, Larach SW, Monson JR (2016) Stereotactic navigation for TAMIS-TME. Minim Invasive Ther Allied Technol 25(5):271–277
7. Wijsmuller AR, Giraudeau C, Leroy J, Kleinrensink GJ, Rociu E, Romagnolo LG, Melani AGF, Agnus V, Diana M, Soler L, Dallemagne B, Marescaux J, Mutter D (2018) A step towards stereotactic navigation during pelvic surgery: 3D nerve topography. Surg Endosc 32(8):3582–3591
8. Wijsmuller AR, Romagnolo LGC, Agnus V, Giraudeau C, Melani AGF, Dallemagne B, Marescaux J (2018) Advances in stereotactic navigation for pelvic surgery. Surg Endosc 32(6):2713–2720
9. Nijkamp J, Kuhlmann K, Sonke JJ, Ruers T (2016) Image-guided navigation surgery for pelvic malignancies using electromagnetic tracking and intra-operative imaging. Int J Comput Assist Radiol Surg 11:S107–S108
10. Atallah S, Tilahun Y, Monson JR (2016) Real-time stereotactic navigation for the laparoscopic excision of a pelvic neoplasm. Tech Coloproctol 20(8):599–600
11. Diana M, Marescaux J (2015) Robotic surgery. Br J Surg 102(2):e15–e28. https://doi.org/10.1002/bjs.9711
12. Pigazzi A, Garcia-Aguilar J (2010) Robotic colorectal surgery: for whom and for what? Dis Colon Rectum 53(7):969–970
13. Atallah S, Martin-Perez B, Pinan J, Quinteros F, Schoonyoung H, Albert M, Larach S (2014) Robotic transanal total mesorectal excision: a pilot study. Tech Coloproctol 18(11):1047–1053
14. Gómez Ruiz M, Parra IM, Palazuelos CM, Martín JA, Fernández CC, Diego JC, Fleitas MG (2015) Robotic-assisted laparoscopic transanal total mesorectal excision for rectal cancer: a prospective pilot study. Dis Colon Rectum 58(1):145–153
15. Kuo LJ, Ngu JC, Tong YS, Chen CC (2017) Combined robotic transanal total mesorectal excision (R-taTME) and single-site plus one-port (R-SSPO) technique for ultra-low rectal surgery-initial experience with a new operation approach. Int J Colorectal Dis 32(2):249–254. https://doi.org/10.1007/s00384-016-2686-3
16. Medina MG, Tsoraides SS, Dwyer AM3 (2018) Review and update: robotic transanal surgery (RTAS). Updates Surg 70(3):369–374
17. Hompes R (2015) Robotics and transanal minimal invasive surgery (TAMIS): the "sweet spot" for robotics in colorectal surgery? Tech Coloproctol 19(7):377–378
18. Huscher CG, Bretagnol F, Ponzano C (2015) Robotic-assisted transanal total mesorectal excision: the key against the Achilles' heel of rectal cancer? Ann Surg 261(5):e120–e121
19. Peters BS, Armijo PR, Krause C, Choudhury SA, Oleynikov D (2018) Review of emerging surgical robotic technology. Surg Endosc 32(4):1636–1655
20. Hughes-Hallett A, Pratt P, Mayer E, Martin S, Darzi A, Vale J (2014) Image guidance for all–TilePro display of 3-dimensionally reconstructed images in robotic partial nephrectomy. Urology 84(1):237–242
21. Woo Y, Choi GH, Min BS, Hyung WJ (2014) Novel application of simultaneous multi-image display during complex robotic abdominal procedures. BMC Surg 15(14):13. https://doi.org/10.1186/1471-2482-14-13
22. Porpiglia F, Checcucci E, Amparore D, Autorino R, Piana A, Bellin A, Piazzolla P, Massa F, Bollito E, Gned D, De Pascale A, Fiori C (2018) Augmented-reality robot-assisted radical prostatectomy using hyper-accuracy three-dimensional reconstruction (HA3DTM) technology: a radiological and pathological study. BJU Int. https://doi.org/10.1111/bju.14549
23. Pessaux P, Diana M, Soler L, Piardi T, Mutter D, Marescaux J (2015) Towards cybernetic surgery: robotic and augmented reality-assisted liver segmentectomy. Langenbecks Arch Surg 400(3):381–385
24. Furukawa J, Miyake H, Tanaka K, Sugimoto M, Fujisawa M (2014) Console-integrated real-time three-dimensional image overlay navigation for robot-assisted partial nephrectomy with selective arterial clamping: early single-centre experience with 17 cases. Int J Med Robot 10(4):385–390
25. Long JA, Lee BH, Guillotreau J, Autorino R, Laydner H, Yakoubi R, Rizkala E, Stein RJ, Kaouk JH, Haber GP (2012) Real-time robotic transrectal ultrasound navigation during robotic radical prostatectomy: initial clinical experience. Urology 80(3):608–613
26. Kenngott HG, Wegner I, Neuhaus J, Nickel F, Fischer L, Gehrig T, Meinzer HP, Müller-Stich BP (2013) Magnetic tracking in the operation room using the da Vinci(®) telemanipulator is feasible. J Robot Surg 7:59–64
27. Marescaux J, Diana M (2015) Inventing the future of surgery. World J Surg 39(3):615–622
28. Atallah S, Zenoni S, Kelly J, Tilahun Y, Monson JR (2016) A blueprint for robotic navigation: pre-clinical simulation for transanal total mesorectal excision (taTME). Tech Coloproctol 20(9):653–654
29. Spiegel EA, Wycis HT, Marks M, Lee AJ (1947) Stereotaxic apparatus for operations on the human brain. Science 106(2754):349–350
30. Willems PW, van der Sprenkel JW, Tulleken CA, Viergever MA, Taphoorn MJ (2006) Neuronavigation and surgery of intracerebral tumours. J Neurol 253(9):1123–1136
31. Willems PW, Taphoorn MJ, Burger H, Berkelbach van der Sprenkel JW, Tulleken CA (2006) Effectiveness of neuronavigation in resecting solitary intracerebral contrast-enhancing tumors: a randomized controlled trial. Neurosurg 104(3):360–368
32. Wirtz CR, Albert FK, Schwaderer M et al (2000) The benefit of neuronavigation for neurosurgery analyzed by its impact on glioblastoma surgery. Neurol Res 22:354–360
33. Kurimoto M, Hayashi N, Kamiyama H, Nagai S, Shibata T, Asahi T, Matsumura N, Hirashima Y, Endo S (2004) Impact of neuronavigation and image-guided extensive resection for adult patients with supratentorial malignant astrocytomas: a single-institution retrospective study. Minim Invasive Neurosurg 47(5):278–283
34. Franchini Melani AG, Diana M, Marescaux J (2016) The quest for precision in transanal total mesorectal excision. Tech Coloproctol 20(1):11–18
35. Rullier E (2015) Transanal mesorectal excision: the new challenge in rectal cancer. Dis Colon Rectum 58(7):621–622
36. Atallah S (2015) The dawn of the digital operating theatre and the rise of the digital surgeon. Tech Coloproctol 19(9):499–501
37. Wagner M, Gondan M, Zöllner Wünscher C, Nickel JJ, Albala F, Groch L, Suwelack A, Speidel S, Maier-Hein S, Müller-Stich L, Kenngott BP HG (2016) Electromagnetic organ tracking allows for real-time compensation of tissue shift in image-guided laparoscopic rectal surgery: results of a phantom study. Surg Endosc 30(2):495–503
38. Arlt F, Chalopin C, Müns A, Meixensberger J, Lindner D (2016) Intraoperative 3D contrast-enhanced ultrasound (CEUS): a prospective study of 50 patients with brain tumours. Acta Neurochir (Wien) 158(4):685–694

39. Lindner D, Trantakis C, Renner C, Arnold S, Schmitgen A, Schneider J, Meixensberger J (2006) Application of intraoperative 3D ultrasound during navigated tumor resection. Minim Invasive Neurosurg 49(4):197–202
40. Jafari MD, Wexner SD2, Martz JE3, McLemore EC, Margolin DA, Sherwinter DA, Lee SW, Senagore AJ8, Phelan MJ, Stamos MJ (2015) Perfusion assessment in laparoscopic left-sided/anterior resection (PILLAR II): a multi-institutional study. J Am Coll Surg 220(1):82–92
41. Boni L, David G, Dionigi G, Rausei S, Cassinotti E, Fingerhut A (2016) Indocyanine green-enhanced fluorescence to assess bowel perfusion during laparoscopic colorectal resection. Surg Endosc 30(7):2736–2742
42. Mizrahi I, Wexner SD (2017) Clinical role of fluorescence imaging in colorectal surgery—a review. Exp Rev Med Dev 14(1):75–82
43. Mizrahi I, de Lacy FB, Abu-Gazala M, Fernandez LM, Otero A, Sands DR, Lacy AM, Wexner SD (2018) Transanal total mesorectal excision for rectal cancer with indocyanine green fluorescence angiography. Tech Coloproctol. https://doi.org/10.1007/s10151-018-1869-z
44. Ris F, Yeung T, Hompes R, Mortensen NJ (2015) Enhanced reality and intraoperative imaging in colorectal surgery. Clin Colon Rectal Surg 28(3):158–164
45. Barnes TG, Volpi D, Cunningham C, Vojnovic B, Hompes R (2018) Improved urethral fluorescence during low rectal surgery: a new dye and a new method. Tech Coloproctol 22(2):115–119
46. Nagata J, Fukunaga Y, Akiyoshi T, Konishi T, Fujimoto Y, Nagayama S, Yamamoto N, Ueno M (2016) Colonic marking with near-infrared, light-emitting, diode-activated indocyanine green for laparoscopic colorectal surgery. Dis Colon Rectum 59(2):e14–e18. https://doi.org/10.1097/DCR.0000000000000542
47. Atallah S, Mabardy A, Volpato AP, Chin T, Sneider J, Monson JRT (2017) Surgery beyond the visible light spectrum: theoretical and applied methods for localization of the male urethra during transanal total mesorectal excision. Tech Coloproctol 21(6):413–424
48. Mondal SB, Gao S, Zhu N, Habimana-Griffin L, Akers WJ, Liang R, Gruev V, Margenthaler J, Achilefu S (2017) Optical see-through cancer vision goggles enable direct patient visualization and real-time fluorescence-guided oncologic surgery. Ann Surg Oncol 24(7):1897–1903
49. Stummer W, Pichlmeier U, Meinel T, Wiestler OD, Zanella F, Reulen HJ, ALA-Glioma Study Group (2006) Fluorescence-guided surgery with 5-aminolevulinic acid for resection of malignant glioma: a randomised controlled multicentre phase III trial. Lancet Oncol 7(5):392–401
50. Ng WP, Liew BS, Idris Z, Rosman AK (2017) Fluorescence-guided versus conventional surgical resection of high grade glioma: a single-centre, 7-year, comparative effectiveness study. Malays J Med Sci 24(2):78–86
51. Jones JE, Busi SB, Mitchem JB, Amos-Landgraf JM, Lewis MR (2018) Evaluation of a tumor-targeting, near-infrared fluorescent peptide for early detection and endoscopic resection of polyps in a rat model of colorectal cancer. Mol Imaging. https://doi.org/10.1177/1536012118790065
52. Kim J, Do EJ, Moinova H, Bae SM, Kang JY, Hong SM, Fink SP, Joo J, Suh YA, Jang SJ, Hwang SW, Park SH, Yang DH, Ye BD, Byeon JS, Choe J, Yang SK, Markowitz SD, Kim SY, Myung SJ (2017) Molecular imaging of colorectal tumors by targeting colon cancer secreted protein-2 (CCSP-2). Neoplasia 19(10):805–816
53. Schiemer JF, Zimniak L, Hadzijusufovic E, Lang H, Kneist W (2018) Novel multi-image view for neuromapping meets the needs of the robotic surgeon. Tech Coloproctol 22(6):445–448
54. Schiemer JF, Zimniak L, Grimminger P, Lang H, Kneist W (2018) Robot-guided neuromapping during nerve-sparing taTME for low rectal cancer. Int J Colorectal Dis. https://doi.org/10.1007/s00384-018-3126-3
55. Chand M, Ramachandran N, Stoyanov D, Lovat L (2018) Robotics, artificial intelligence and distributed ledgers in surgery: data is key! Tech Coloproctol 22(9):645–648
56. Guerriero L, Quero G, Diana M, Soler L, Agnus V, Marescaux J, Corcione F (2018) Virtual reality exploration and planning for precision colorectal surgery. Dis Colon Rectum 61(6):719–723
57. Schols RM, Bouvy ND, van Dam RM, Stassen LP (2013) Advanced intraoperative imaging methods for laparoscopic anatomy navigation: an overview. Surg Endosc 27(6):1851–1859. https://doi.org/10.1007/s00464-012-2701-x